

Quasineutral plasma models

R. F. Fernsler and S. P. Slinker

Plasma Physics Division, Naval Research Laboratory, Washington, DC 20375, USA

G. Joyce

Icarus Research Inc., Bethesda, Maryland 20824, USA

(Received 13 September 2004; published 4 February 2005)

The quasineutral plasma model proposed by Langmuir more than 75 years ago is still widely used today and is based on two approximations: charge neutrality and the Boltzmann relationship for electrons. However, the Boltzmann relationship is unnecessary and is not always justified. Moreover, because the Boltzmann relationship is fluid based, it compromises kinetic treatments and gives rise to troublesome singularities in the Bohm condition. To overcome these limitations, more general quasineutral models are developed. Two of the models are fluid based while the third is fully kinetic. The kinetic model and one of the fluid models lead directly to the Bohm condition, but without the singularities seen earlier. Fluid simulations are presented to test and compare the various approaches.

DOI: 10.1103/PhysRevE.71.026401

PACS number(s): 52.25.Dg, 52.25.Fi, 52.27.Cm

I. INTRODUCTION

Many of today's plasma models date back to the seminal work done by Langmuir [1,2] more than 75 years ago. Langmuir recognized that plasmas are sufficiently good electrical conductors that the electrostatic field in the interior can be determined without solving Poisson's equation. The plasma frequency ω_p , conductivity σ , and Debye length λ_D are then no longer relevant as scale parameters, so numerical solutions can be formulated around macroscopic temporal and spatial scales instead [3,4]. Because the macroscopic and plasma scales can differ by many orders of magnitude, avoiding Poisson's equation is not only useful but often essential [5]. Poisson's equation is needed, of course, to describe the highly charged sheaths that form at the boundaries.

Langmuir obtained the electrostatic field from the electron density using the Boltzmann relationship, and he obtained the electron density from the ion densities by setting the charge density to zero in the plasma interior. Tonks and Langmuir [2] showed the latter assumption is justified as long as the electric field varies slowly over the plasma screening distance. That property is the basis for quasineutrality.

However, while the Boltzmann relationship simplifies quasineutral modeling, it is unnecessary and not always valid. It fails, for example, in plasmas that are strongly magnetized or highly electronegative [6], and it fails in dc discharges where Ohm's law usually gives better (and fundamentally different) results. In addition, because the Boltzmann relationship is fluid based, it compromises kinetic analysis and leads to unphysical singularities in the Bohm condition when the ions are treated kinetically [7–10].

Some of these limitations can be overcome by using the electron momentum equation in place of the Boltzmann approximation, and this approach has been tried at various levels of approximation [3,4,6]. However, even these models fail in electron-free (ion-ion) plasmas, so we first derive a field equation based on all the momentum equations. Like Langmuir, we then replace Poisson's equation with the as-

sumption that the charge density is small. While this model has a wide range of validity, it reveals little about the screening ability of the plasma. The model also has no direct analog in kinetic theory.

The major goal of the present work is to derive quasineutral models, in both kinetic [11] and fluid [12] forms, directly from Poisson's equation (Gauss's law). These models treat all species equally and account for the plasma current in full. While the fluid version is not necessarily more accurate than previous models, it more clearly reveals the physical basis and limitations of quasineutrality. The kinetic version is actually easier to derive, and it gives the quasineutral field in terms of a set of velocity integrals. Both formulations lead directly to the Bohm condition, and the integrals in the kinetic version are inherently nonsingular, unlike in previous work [7–10]. Both models are derived by using the derivative of Gauss's law to obtain a higher-order field equation in terms of a plasma screening distance. The full equation reduces to an algebraic expression in regions where the field varies slowly over the screening distance, and the validity of the quasineutral expression can be assessed by examining the terms dropped. Underlying the analysis is the assumption that the plasma varies along one direction only and slowly in time relative to ω_p and $4\pi\sigma$. To validate the overall concept, we compare fluid solutions from the various quasineutral models with the solution from Poisson's equation. The solutions differ, sometimes radically, from one another and from traditional plasma theory.

The paper is organized as follows. After briefly reviewing why sheaths form, a general set of fluid equations is presented. These equations serve as the basis for two different quasineutral models, the second of which leads directly to a Bohm condition similar to that derived by Riemann [9]. A fully kinetic treatment is presented in Sec. III. In Sec. IV we compare the various fluid models. We describe the effects of a perpendicular magnetic field in Appendix A and give a closed-form solution for a magnetized discharge in Appendix B. Characteristic time scales are discussed in Appendix C.

II. FLUID ANALYSIS

A. Background

To understand why plasmas charge and sheaths form, consider a wall located at x_w . If the wall emits few or no particles, kinetic theory indicates that each plasma species i flows into the wall with a mean velocity satisfying

$$u_i(x_w) \geq \chi_i \sqrt{\frac{g_i T_i}{m_i}}. \quad (1)$$

Here T_i is the species temperature (in units of energy), m_i is the species mass, $g_i < 1$ is a numerical factor determined by the velocity distribution, and χ_i is a sticking coefficient lying between zero (total reflection) and unity (total absorption). For charged species impinging on surfaces $\chi_i \approx 1$, while for Maxwellian distributions $g_i = 1/2\pi$. These values are used in the analysis below for convenience.

In the absence of an electric field, condition (1) is an equality and species arrive at the wall with flow velocities u_i determined by the thermal speeds $\sqrt{T_i/m_i}$. If the wall is an insulator, the net current quickly approaches zero, $\sum_i e q_i n_i u_i \rightarrow 0$, while the plasma densities n_i adjust to allow for the differences in u_i . The charge density is then nonzero, $\rho = \sum_i e q_i n_i \neq 0$, where $-e$ is the electron charge and $q_i e$ is the charge of species i . The plasma charge ρ generates an electrostatic field that reduces but does not eliminate the differences in u_i .

As shown later, quasineutrality is justified only in regions where ρ is small relative to the total positive and total negative charge densities separately. This requirement can be expressed as

$$|\rho| \ll \sum_i |q_i| e n_i. \quad (2)$$

Condition (2) is well met in the interior of dense plasmas (where the flow velocities approach zero), but it is met at the boundaries only if the thermal velocities $\sqrt{T_i/m_i}$ are comparable for all major species. Hence, while quasineutrality can apply throughout ion-ion plasmas [13], it invariably fails near the boundaries of electron-rich plasmas, because T_i/m_i is much larger for electrons than ions.

B. Fluid equations

Assume all parameters vary along direction \hat{s} only. Temporarily neglecting magnetic forces, the continuity and momentum equations for species i then reduce to

$$\frac{\partial n_i}{\partial t} + \frac{1}{A} \frac{\partial}{\partial s} (n_i u_i A) = S_i \quad (3a)$$

and

$$n_i m_i \frac{\partial u_i}{\partial t} + n_i m_i u_i \frac{\partial u_i}{\partial s} = q_i e E n_i - \frac{\partial (n_i T_i)}{\partial s} - n_i m_i u_i R_i, \quad (3b)$$

respectively. Here S_i is the net production rate for the species, R_i is the rate at which the species loses momentum to collisions of any type, E is the electric field, and $A(s)$ char-

acterizes the plasma area. For planar flow $A(s)=1$, for cylindrical flow $A(s)=2\pi s$, and for spherical flow $A(s)=4\pi s^2$. In the latter two cases, s measures the distance from the center of curvature.

Other variations in $A(s)$ are possible and can be produced, for example, by using a longitudinal magnetic field $B(s)\hat{s}$ that varies with s . Indeed, a rapidly diverging magnetic field can be used to accelerate [14,15] quasineutral plasmas to velocities above the ion sound speed $c_s \approx \sqrt{T_e/m_p}$. Here T_e is the electron temperature and m_p is the positive-ion mass. However, Eq. (3b) still applies, because the magnetic mirror force along \hat{s} is small, as long as collisions keep the electron pressure nearly isotropic [4]. Moreover, if the magnetic field is instead perpendicular to \hat{s} , the magnetic forces along s can often be incorporated simply by modifying the momentum-loss rates R_i , as shown in Appendix A. Equations (3a) and (3b) thus have a wide range of applicability.

The electric field E lies along \hat{s} as well in this case and obeys Gauss's law,

$$\frac{1}{A} \frac{\partial (EA)}{\partial s} = 4\pi\rho = 4\pi e \sum_i q_i n_i. \quad (4)$$

However, as mentioned earlier, the goal of quasineutrality is to replace this differential equation with an algebraic approximation in the plasma interior where ρ is small. The next several sections outline various approaches toward that goal.

C. Langmuir model

Langmuir replaced Eq. (4) with the Boltzmann relationship for electrons,

$$eE = - \frac{T_e}{n_e} \frac{\partial n_e}{\partial s}, \quad (5)$$

and he obtained the electron density n_e from the ion densities by setting $\rho=0$ in the plasma interior. However, while Eq. (5) is widely used, it is not always justified. Let us therefore first determine when Eq. (5) and the Langmuir model apply.

To understand the basis for Eq. (5), assume $\partial/\partial t=0$ for simplicity and use the last term in Eq. (3b) to compute the current densities $e q_i n_i u_i$. Then set the sum of the current densities equal to the total current density $J=I_c/A$, and extract the electric field to obtain

$$E = \frac{I_c/A + \sum_i \frac{e q_i}{m_i R_i} \left[\frac{\partial (n_i T_i)}{\partial s} + \frac{n_i}{2} \frac{\partial (m_i u_i^2)}{\partial s} \right]}{\sum_i \frac{e^2 q_i^2 n_i}{m_i R_i}}. \quad (6)$$

This equation is exact, given the assumptions made.

The net current I_c flowing through area A is uniform in steady state, $\partial I_c/\partial s=0$, and satisfies Ohm's law $I_c = \sigma EA$ if the plasma itself is uniform ($\partial/\partial s=0$). Ohm's law is a good approximation when the flow is mobility limited (as in dc discharges) but not when the flow is driven by particle pressure instead (e.g., when $I_c=0$). Rogoff [16] and others [17,18] gave similar expressions for E , but without I_c or the

inertial terms. Any current flowing through the plasma then affects the electron flow velocity u_e only, as is true in the Langmuir model as well. According to Eq. (6), however, the current affects the field E and thus the velocities and densities of all species.

The electron temperature usually varies weakly with s and satisfies $T_e \gg m_e u_e^2$ by virtue of Eq. (1). Equation (5) is therefore justified provided I_c is small and electrons control both the numerator and denominator of Eq. (6). The denominator equals the dc conductivity σ and is controlled by electrons only if

$$n_e \mu_e \gg \sum_{i \neq e} |q_i| n_i \mu_i, \quad (7)$$

where $\mu_i \equiv |eq_i/m_i R_i|$ is the effective mobility of species i and the subscript e denotes electrons. This condition is well satisfied in unmagnetized, electropositive plasmas, because in those plasmas $n_i \leq n_e$ and $\mu_i \leq 10^{-2} \mu_e$ for all $i \neq e$.

In electronegative plasmas, however, the ion densities can exceed n_e , and condition (7) is then met only if the total negative-ion density satisfies $n_n \ll (\mu_e/\mu_i)n_e$ for all $i \neq e$. Similarly, as outlined in Appendixes A and B, a magnetic field B perpendicular to \hat{s} increases the effective collision frequency R_i far more for electrons than ions [6], and consequently condition (7) is met only if the electron cyclotron frequency is modest, $\Omega_e \equiv eB/m_e c \ll \sqrt{\nu_e \nu_i} m_i/m_e$ for all $i \neq e$. Here ν_i is the momentum-transfer collision frequency of species i . The magnetic condition translates to $B/P < 1$ G/mtorr in electropositive gases like nitrogen, but a stronger condition is needed if the gas is electronegative: $(B/P)(n_p/n_e) < 1$ G/mtorr. Here P is the equivalent gas pressure at room temperature and n_p is the total positive-ion density.

The above limitations can be avoided by using Eq. (6) in place of the Boltzmann relationship (5). Quasineutrality must still be imposed, however, both to represent Poisson's equa-

tion and to keep the charge density from growing unphysically [4]. To do so, compute the densities and velocities of all species save one, using Eqs. (3). Then use charge neutrality

$$n_k = -q_k^{-1} \sum_{i \neq k} q_i n_i \quad (8a)$$

and current conservation

$$u_k = \frac{1}{q_k n_k} \left[\frac{I_c}{eA} - \sum_{i \neq k} q_i n_i u_i \right] \quad (8b)$$

to compute the density and velocity of the last species k . Condition (8b) is not actually needed but simplifies the calculations.

As an aside, we note that the Boltzmann relationship is sometimes used for negative ions as well [18–21], even though they do not satisfy a condition equivalent to Eq. (7). This treatment is nevertheless justified, provided the negative ions are nearly collisionless [18] and carry little current. The underlying physics is therefore different and of little interest here.

D. Different approach

Like the Boltzmann relationship, Eq. (6) gives no measure of plasma screening, even though it applies in regions where the plasma is non-neutral. To overcome that limitation, we now derive a higher-order field equation. Time derivatives are retained as well, mainly to allow for currents and voltages that vary with time.

To derive the higher-order equation, first eliminate the velocity gradients $\partial u_i / \partial s$ from Eqs. (3a) and (3b). The density gradients are then given by

$$\frac{\partial n_i}{\partial s} = \frac{q_i e E n_i - m_i u_i (n_i R_i + S_i) - n_i \frac{\partial T_i}{\partial s} + n_i m_i u_i^2 \frac{d \ln(A)}{ds} + m_i \left(u_i \frac{\partial n_i}{\partial t} - n_i \frac{\partial u_i}{\partial t} \right)}{T_i - m_i u_i^2}. \quad (9)$$

To eliminate those gradients, multiply by $4\pi e q_i$ and sum over all i . Then combine the sum with the spatial derivative of Gauss's law (4) to produce

$$\nabla^2 E \equiv \frac{\partial}{\partial s} \left[\frac{1}{A} \frac{\partial(EA)}{\partial s} \right] = 4\pi \frac{\partial \rho}{\partial s} = k_s^2 E - Q_c, \quad (10a)$$

where

$$k_s^2 \equiv 4\pi e^2 \sum_i \left(\frac{q_i^2 n_i}{T_i - m_i u_i^2} \right), \quad (10b)$$

$$Q_c \equiv 4\pi e \sum_i \frac{q_i P_i}{T_i - m_i u_i^2}, \quad (10c)$$

and

$$P_i \equiv m_i u_i (n_i R_i + S_i) + n_i \frac{\partial T_i}{\partial s} - n_i m_i u_i^2 \frac{d \ln(A)}{ds} + m_i \left(u_i \frac{\partial n_i}{\partial t} - n_i \frac{\partial u_i}{\partial t} \right). \quad (10d)$$

These equations are as valid as Gauss's law but are more

complicated and of higher order. They thus have no immediate utility.

In the plasma interior, however, the charge density ρ is small by assumption, so $\partial\rho/\partial s$ is small as well. Dropping that term from Eq. (10a) leaves the algebraic result

$$E = \frac{Q_c}{k_s^2}. \quad (11a)$$

This expression, which is the key result of the paper, is justified in regions where the field E varies slowly over the “screening distance” $|k_s|^{-1}$ or slowly relative to changes in k_s^2 . The general requirement is thus

$$\left| \frac{\nabla^2 E}{E} \right| \ll |k_s^2| \quad (11b)$$

or

$$\left| \frac{1}{E} \frac{\partial}{\partial s} \nabla^2 E \right| \ll \left| \frac{\partial k_s^2}{\partial s} \right|. \quad (11c)$$

The last two conditions are the basis for quasineutrality.

To understand that basis better, consider the screening parameter k_s^2 as given by Eq. (10b). This parameter is closely related to the plasma Debye length λ_D defined by

$$\lambda_D^{-2} \equiv 4\pi e^2 \sum_i \frac{q_i^2 n_i}{T_i}, \quad (12)$$

and indeed $k_s^2 = \lambda_D^{-2}$ if the flow velocities $u_i = 0$. If Eq. (10a) were used to compute E , the screening distance $|k_s|^{-1}$ would have to be resolved or at least taken into account. In the plasma interior, however, the field varies so slowly that Eq. (11a) is sufficient and $|k_s|^{-1}$ is no longer relevant as a length scale. Note that $|k_s|^{-1}$ depends strongly [22] on the flow velocities u_i . For example, if the plasma is electron rich and the ions are colder than the electrons, $|k_s|^{-1}$ approaches the ion Debye length in the plasma middle (where $u_i \rightarrow 0$) but approaches the electron Debye length near the boundaries (where $u_i \rightarrow c_s$).

Equation (11a) was derived by assuming ρ and $\partial\rho/\partial s$ are small. To enforce this assumption, set $\rho = 0$ for all s and compute the density of one species k using Eq. (8a) as before. Moreover, because $\partial\rho/\partial t = 0$, we can impose current continuity $\partial I_c/\partial s = 0$, and again use Eq. (8b) to compute the flow velocity u_k of that species. These tactics stabilize and accelerate the calculations. As indicated in Appendix C, current continuity is justified as long as the plasma evolves slowly relative to $4\pi\sigma$ and ω_p , where σ is the dc conductivity and ω_p is the plasma frequency.

E. Singularities and the Bohm condition

Several singularities are evident in Eqs. (10b)–(11a). Some of the singularities are inherent to quasineutrality, while others are easily eliminated and appear in the fluid model only. The fundamental singularities are buried in Eq. (6) as well, of course, and in that sense the present model is more transparent. To understand the singularities, consider the plot of $k_s^2(x)$ shown in Fig. 1(a) for a planar plasma

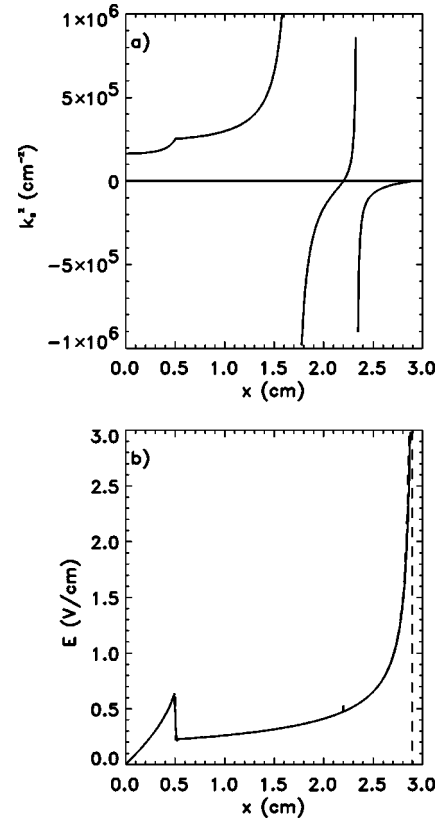


FIG. 1. Plasma produced by an external ionization source (an electron beam) that is uniform from -0.5 to $+0.5$ cm in a gas comprised of 5 mtorr He and 5 mtorr Ar. (a) Screening parameter $k_s^2(x)$. (b) Electric field $E(x)$ from Poisson's equation (solid curve) and from Eq. (13) (dashed curve).

consisting of electrons and two species of positive ions. These results were obtained using Poisson's equation and are valid to order $m_e u_e^2 / T_e \ll 1$, as discussed in Appendix C. According to Eqs. (10b) and (10c), k_s^2 and Q_c diverge and change sign when the flow velocity of a species equals its thermal speed $u_i = \pm \sqrt{T_i/m_i}$. In Fig. 1(a), for example, one ion species (Ar^+) reaches its thermal speed at $x \approx 1.7$ cm, while the second (He^+) does so at $x \approx 2.32$ cm; at each location k_s^2 diverges. Although this divergence is an artifact of the fluid model (as shown in Sec. IV C), condition (11b) is fully met, and thus Eq. (11a) is “exact.” The thermal singularities can therefore be eliminated by rewriting Eq. (11a) as

$$eE = \frac{\sum_i q_i P_i \prod_{j \neq i} (T_j - m_j u_j^2)}{\sum_i \left[\frac{q_i^2 n_i \prod_{j \neq i} (T_j - m_j u_j^2)}{T_i} \right]}. \quad (13)$$

Equation (13) is singular only if the denominator vanishes, because the numerator is now everywhere finite. However, the denominator can and does vanish at multiple locations in plasmas containing more than two species, because $k_s^2 = 0$ between each pair of thermal poles; for example, $k_s^2 = 0$ at $x = 2.2$ and 2.9 cm in Fig. 1(a). Nevertheless, the field E remains finite (and the plasma remains quasineutral) at all but the last location, because the numerator of Eq. (13) van-

ishes as well. To show this [23], assume the flow velocities u_i increase monotonically with distance s from the plasma middle. The number of thermal poles is then no greater than the number of species N , so k_s^2 crosses zero $N-1$ times or less [9]. The quasineutrality condition (8a) reduces the number of independent species from N to $N-1$, and therefore the number of independent species equals the number of singularities in Eq. (13). The quasineutral equations thus contain enough degrees of freedom to eliminate all the singularities, depending on the boundary conditions and other constraints; see Appendix B. Quasineutrality fails, of course, once conditions (11b) and (11c) fail, and the failure can be abrupt. In Fig. 1(b), for example, we compare the field E from Poisson's equation (solid curve) with that from Eq. (13) (dashed curve). Except for the glitch at $x=2.2$ cm, the two plots nearly overlap out to the sheath edge, $x_s \cong 2.9$ cm. At x_s the quasineutral field diverges and quasineutrality fails. The glitch at 2.2 cm occurs because the numerator and denominator of Eq. (13) pass through zero at slightly different locations when Poisson's equation is used.

The Bohm condition represents the one true singularity in Eq. (13), and it consists of *two* requirements:

$$k_s^2(x_s) = 4\pi e^2 \sum_i \frac{q_i^2 n_i}{T_i - m_i u_i^2} = 0 \quad (14a)$$

and

$$Q_c(x_s) \neq 0. \quad (14b)$$

These two requirements define the boundary within which quasineutrality applies, and the first requirement reduces to the Bohm condition as given by Riemann [9] when $m_e u_e^2 / T_e \rightarrow 0$. Since $m_e u_e^2 \ll T_e$ in practice, the main difference between the two models is the addition of requirement (14b). As already mentioned, that requirement eliminates all but one of the locations where Eq. (14a) is satisfied.

Bohm [24] derived the equivalent of condition (14a) by assuming that the plasma area A and temperatures T_i are constant and that no collisions occur inside the sheaths. In that case $Q_c=0$ in the sheaths and Eq. (10a) reduces to

$$\frac{d^2 E}{ds^2} \rightarrow k_s^2 E. \quad (15)$$

This equation shows that the field E grows monotonically with s near the edge of a collisionless sheath only if $k_s^2(x_s) \geq 0$. That requirement is a restatement of the Bohm condition [7,9,25]. The quasineutral model applies only if $d^2 E / ds^2 \rightarrow 0$, however, and thus the quasineutral boundary condition at the edge of a collisionless sheath is $k_s^2 \rightarrow 0$.

III. KINETIC ANALYSIS

A. Plasma screening

Tonks and Langmuir [2] treated the ions kinetically but treated the electrons as a fluid using the Boltzmann relationship. Taking the electron temperature T_e to be constant, they then expanded Poisson's equation from the plasma middle to obtain

$$\begin{aligned} \nabla^2 \phi &= 4\pi(en_e - \rho_{ion}) = 4\pi \left[en_{e0} \exp\left(\frac{e\phi}{T_e}\right) - \rho_{ion} \right] \\ &= 4\pi(en_{e0} - \rho_{ion}) + \left(\frac{4\pi e^2 n_{e0}}{T_e} \right) \phi + \dots \end{aligned} \quad (16)$$

Here ϕ is the electrostatic potential measured from the middle, n_{e0} is the electron density in the middle, and ρ_{ion} is the ion charge density. The term $\nabla^2 \phi$ is negligible in regions where ϕ varies slowly over the electron Debye length $\lambda_{De} = \sqrt{T_e / 4\pi e^2 n_{e0}}$, and in those regions quasineutrality is justified [26] and $e\phi(s) \approx T_e \ln[\rho_{ion}(s) / en_{e0}]$.

B. Fully kinetic model

A fully kinetic model can be obtained by dropping the Boltzmann relationship as before. Assuming the electric field is along \hat{s} and neglecting the magnetic field for simplicity, the kinetic Boltzmann equation for species i is given by

$$\frac{\partial f_i}{\partial t} + v_s \frac{\partial f_i}{\partial s} + \frac{q_i e E}{m_i} \frac{\partial f_i}{\partial v_s} = C_i. \quad (17)$$

Here the velocity distributions f_i depend on the longitudinal velocity v_s , the transverse velocity v_\perp , the spatial coordinate s , and time t only. The velocity distributions and collision cross sections determine the collision operators C_i .

Gauss's law is given in this case by

$$\frac{1}{A} \frac{\partial(EA)}{\partial s} = 4\pi \rho(s,t) = 4\pi e \sum_i q_i \int \int d^2 v_\perp \int_{-\infty}^{\infty} dv_s f_i. \quad (18)$$

Taking the derivative of this equation and obtaining $\partial f_i / \partial s$ from Eq. (17), we find that

$$\begin{aligned} \nabla^2 E &= 4\pi e \sum_i q_i \int \int d^2 v_\perp \int_{-\infty}^{\infty} dv_s \frac{\partial f_i}{\partial s} \\ &= k_s^2 E - Q_c, \end{aligned} \quad (19a)$$

where the screening and source parameters are now given by

$$k_s^2 = -4\pi e^2 \sum_i \frac{q_i^2}{m_i} \int \int d^2 v_\perp \int_{-\infty}^{\infty} dv_s \frac{1}{v_s} \frac{\partial f_i}{\partial v_s} \quad (19b)$$

and

$$Q_c = -4\pi e \sum_i \int \int d^2 v_\perp \left[\int_{-\infty}^{\infty} dv_s \frac{C_i}{v_s} - \frac{\partial}{\partial t} \int_{-\infty}^{\infty} dv_s \frac{f_i}{v_s} \right]. \quad (19c)$$

Equations (19) are the analogs of Eqs. (10) and again yield

$$E \rightarrow \frac{Q_c}{k_s^2}, \quad (20)$$

in regions where the quasineutrality conditions (11b) and (11c) are met. As before, the time derivatives in Eq. (19c) are usually important only if the current varies with time.

Equations (19b)–(20) constitute a complete, kinetic model for the quasineutral electric field. While each species is normally followed separately, quasineutrality must again be imposed, because Eq. (20) applies only in that limit. The density of one species should therefore be renormalized to satisfy Eq. (8a) before using Eqs. (19b) and (19c). However, the current-continuity condition (8b) is impractical (and unnecessary) in this case, because the velocity distributions are difficult to adjust. Hence, specify the current only at the boundaries, using a procedure like that outlined in Ref. [4] for collisionless sheaths. In particular, the potential drop across a collisionless sheath determines whether particles of a given charge and velocity pass through the sheath or reflect off it. Particles reflecting off the sheath reenter the quasineutral plasma with their velocities reversed, and thus the potential at each sheath can be adjusted until the total plasma current equals $I_c(t)$. The velocity distributions inside the plasma respond to those at the boundaries through the convective term in Eq. (17), so $\partial I_c / \partial s \rightarrow 0$ automatically. Note that this method yields the voltage across each sheath (and thus the final ion energies) without explicitly modeling the sheath [4].

C. Bohm condition

The velocity distributions f_i are positive, and they fall off faster than v_s^{-1} at $v_s = \pm\infty$ since the plasma densities are finite. In addition, the distributions are analytic at $v_s = 0$ due to smoothing by collisions and other processes. The derivatives $\partial f_i / \partial s$ and collision operators C_i have the same properties, and thus k_s^2 and Q_c are finite everywhere, despite the pole in Eqs. (19b) and (19c). Hence, unlike the fluid model, the kinetic model is singular *only* when the Bohm condition is met: $k_s^2 = 0$ and $Q_c \neq 0$. As before, this condition applies at the boundaries only, if at all.

Previous kinetic expressions for the Bohm condition are similar, except the poles are one order higher [7–10]. For example, Riemann [9,10] obtained the form

$$\sum_{i \neq e} \frac{q_i}{m_i} \int \int d^2 v_{\perp} \int_{-\infty}^{\infty} dv_s \frac{f_i}{v_s^2} = \frac{1}{m_e} \int \int d^2 v_{\perp} \int_{-\infty}^{\infty} dv_s \frac{1}{v_s} \frac{\partial f_e}{\partial v_s}.$$

This form confirms the kinetic result obtained earlier by Harrison and Thompson [7], and it can be derived by integrating Eq. (19b) by parts for $i \neq e$. Riemann [10] showed that this form of the Bohm condition is met only if the positive ions acquire a mean velocity no less than the sound speed c_s . However, integration by parts is justified only if $f_i = 0$ at $v_s = 0$, and that requirement is met only for species that are driven toward the walls by the field E and are neither produced nor suffer collisions within the sheaths. For all other species (and for actual sheaths in general), $f_i \neq 0$ at $v_s = 0$ and

the integrals should then be left in their original form (with a simple pole only).

IV. SIMULATIONS

To test the various models, we compared the electric field as given by Eqs. (5), (6), and (13) with that from Poisson's equation for three planar problems in x . The walls in each case were located at $x = \pm 3$ cm and were held at zero potential. To produce strong spatial variations in the electric field (and to avoid the eigenvalue problem discussed in Appendix B), we took the gas ionization rate to be constant from -0.5 to $+0.5$ cm and zero elsewhere. The rate was based on the ionization generated by a 3 keV electron beam [27–31] propagating in y . For beam-produced plasmas, the electron temperature T_e ranges from ~ 0.5 eV in molecular gases to ~ 1 eV in rarefied noble gases [28–30], and these values were used in the simulations. The collision frequencies and rate coefficients were derived from data compiled by Dutton [32], Ellis *et al.* [33], and Christophorou and Olthoff [34].

Equations (3) were first solved as functions of time using Poisson's equation, condition (1), and the adjustments described in Appendix C. The code was run until equilibrium was reached, $I_c \rightarrow 0$. Resolving the sheath required a small grid size $\Delta x \ll \lambda_{De}$, which in turn required a small time step $\Delta t < \lambda_{De} \sqrt{2\pi m_e / T_e}$, based on the Courant criterion. Here λ_{De} is the electron Debye length and $\sqrt{T_e / 2\pi m_e}$ is the electron flow velocity at the walls. Additional restrictions on Δt are discussed in Appendix C.

We next inserted the ion solutions obtained with Poisson's equation into Eqs. (8) to determine the quasineutral electron density $n_e(x)$ and flow velocity $u_e(x)$. These values were close to the original values, except near the walls. The new values were then inserted into Eq. (5), (6), or (13) to determine the quasineutral field $E(x)$. Results from Eqs. (6) and (13) were largely indistinguishable, so only those from Eq. (13) are shown.

The quasineutral models were also run in time, but with limited success. In particular, solutions based on Eq. (13) were often unstable in plasmas containing more than two species, because of the singularities at $k_s^2 = 0$. In simpler plasmas the solutions were stable and agreed well with the solutions from Poisson's equation up to the sheath edge. Solutions based on Eq. (5) or (6) were more robust in general, but those from Eq. (5) did not always agree with the solutions to Poisson's equation.

A. Two species of positive ions

The example cited in Sec. II E describes a plasma nominally formed in a mixture of 5 mtorr Ar and 5 mtorr He. The magnetic field was zero, T_e was 1 eV, and the temperatures of Ar^+ and He^+ were set to 0.25 eV to highlight the singularities. Apart from the glitch at 2.2 cm (where $k_s^2 = 0$), the electric field from Eq. (13) agreed well with that from Poisson's equation up to the sheath edge, $x_s \approx 2.9$ cm; see Fig. 1(b). The field from Eq. (5) agreed equally well in this case but without the glitch.

In the simulation, the He^+ ions were lighter but had a higher collision frequency than Ar^+ . The flow velocity u_i was therefore greater for He^+ , but the drift energy $m_i u_i^2/2$ was larger for Ar^+ . As a result, the Bohm condition was met when $u_i > c_i$ for Ar^+ but $u_i < c_i$ for He^+ , where $c_i \equiv \sqrt{(T_e + T_i)/(m_e + m_i)}$ is the sound speed of species i . This result is consistent with claims made by Severn *et al.* [35] and Franklin [36].

B. Electronegative plasma

Now consider two problems where the Boltzmann relationship (5) is *not* justified. In the first problem the gas consisted of 1 torr He plus a trace amount ($\sim 0.1\%$) of the highly attaching gas SF_6 . The magnetic field was again zero, T_e was 0.5 eV, and the ion temperatures were set to the gas temperature 0.025 eV. To simplify the calculations, we neglected charge exchange, took ion-ion recombination as the sole loss mechanism, and assumed the plasma consisted of electrons (e) and He^+ (p) and $\text{SF}_5^-(n)$ ions only. Given those assumptions, most electrons attached to form negative ions before reaching the walls, but not before generating an ambipolar electric field that pushed negative ions toward the plasma middle and positive ions toward the walls. The negative ions therefore accumulated in the middle until they recombined with positive ions. As a result, the ion densities became large [17,18,37] in the middle: $n_n \approx n_p \sim 50n_e$. See Fig. 2(a).

Using the ion densities and velocities obtained with Poisson's equation, we recomputed the electric field using Eqs. (5) and (13). In Fig. 2(b) the field from Eq. (13) (diamonds) agrees well with that from Poisson's equation (solid curve) up to the sheath edge, $x_s \approx 2.9$ cm, but the field from Eq. (5) (dot-dashed) is too large by nearly 30%. The Boltzmann relationship (and thus the Langmuir model) worked poorly in this case because the electronegativity was large: $n_n/n_e \sim 0.5\mu_e/\mu_p \sim 50$, where μ_p is the mobility of He^+ . Furthermore, using a Boltzmann relationship for the negative ions, $eE = -T_n[d \ln(n_n)/dx]$, gives a field that is nearly two orders of magnitude too small. The Boltzmann relationship is therefore not justified for *any* species in this example.

The ion-neutral collision frequency was so high in this case that the ion flow velocities remained below the sound speed for all x . The Bohm condition was therefore never met and thus is unsuitable as a quasineutral boundary condition.

C. Magnetized plasma

The Boltzmann relationship failed more dramatically yet for the last problem presented. In this case a magnetic field of 100 G was applied along y in 10 mtorr of pure He. The plasma electron temperature was 1 eV and the ion temperature was 0.025 eV. The magnetic field confined the electrons so strongly that they diffused more slowly than the ions, even though the ions were far heavier and colder. As a result, the ambipolar electric field E was negative rather than positive in the plasma middle [6], and E became positive near the walls only after ion inertia became important. The plasma densities therefore peaked as usual in the plasma middle in

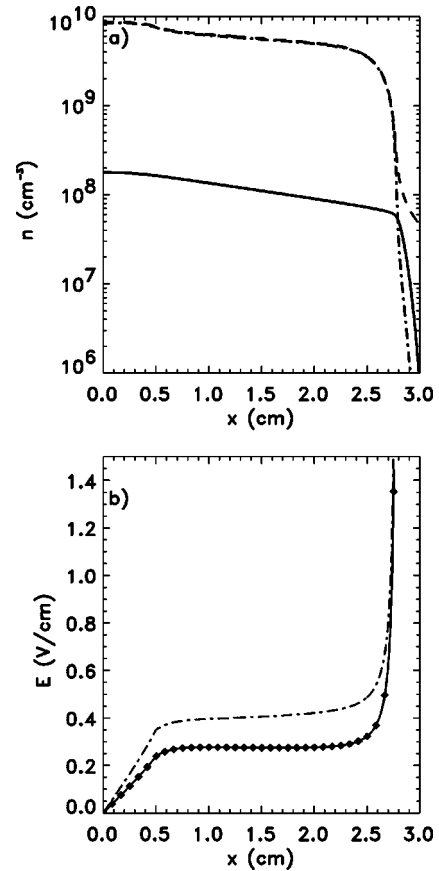


FIG. 2. Beam-produced plasma in 1 torr He plus $\sim 0.1\%$ SF_6 . (a) Density of positive ions (dashed curve), negative ions (dot-dashed curve), and electrons (solid curve). (b) $E(x)$ from Poisson's equation (solid curve), from Eq. (5) (dot-dashed curve), and from Eq. (13) (diamonds).

Fig. 3(a), but the electrostatic potential ϕ peaked off axis and remained well below T_e/e in Fig. 3(b).

Using the ion density and velocity obtained with Poisson's equation, we again recomputed the electric field from Eqs. (5) and (13). In Fig. 3(c) the field from Eq. (13) (diamonds) agrees with that from Poisson's equation (solid curve), but the field from Eq. (5) (dot-dashed curve) is more than two orders of magnitude too large *and* has the wrong sign. This failure results from the inability of the Boltzmann relationship (and thus the Langmuir model) to account for the momentum lost by electrons. See also the analytic solution given in Appendix B for a related problem.

The magnetic field kept the ion flow velocity below the sound speed for all x , as in the previous example. Hence, the Bohm condition was never met and is again not suitable as a quasineutral boundary condition.

V. SUMMARY

Three models were presented to generalize the original quasineutral plasma model proposed by Langmuir. Langmuir's model is based on the Boltzmann relationship for electrons, but that approximation fails in dc discharges and in plasmas that are highly magnetized or electronegative. The

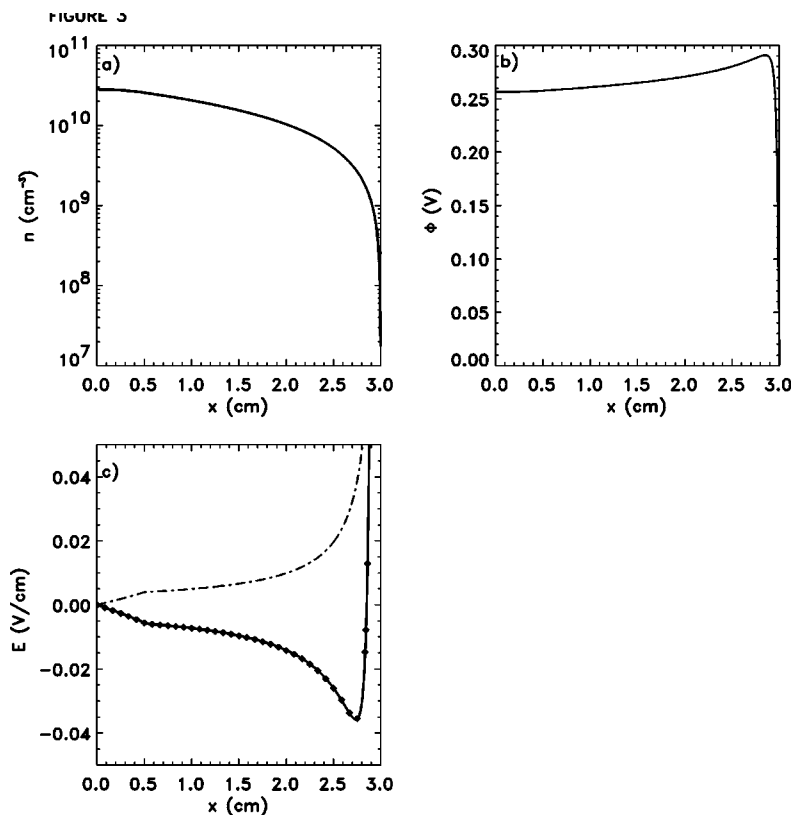


FIG. 3. Beam-produced plasma confined by a 100 G magnetic field in 10 mtorr He. (a) Density of positive ions (dashed curve) and electrons (solid curve). (b) Potential $\phi(x)$. (c) $E(x)$ from Poisson's equation (solid curve), from Eq. (13) (diamonds), and from Eq. (5) (dot-dashed curve) multiplied by 10^{-2} .

models presented here avoid these limitations and are based on two different approaches. The first approach used the momentum equations of all species, not just electrons, to derive a general field equation. Charge neutrality was then imposed, as in the Langmuir model. The second approach used Gauss's law to obtain a higher-order field equation in terms of a plasma screening distance. Quasineutrality was then imposed by assuming the field varies slowly over the screening distance. The second approach does not require fluid equations and was used to derive a fully kinetic model, as well as another fluid model. Both of these models lead directly to the Bohm condition, but without the singularities seen in previous kinetic analyses. However, the last two models contain removable singularities that must be treated properly to obtain stable numerical solutions.

To test the various approaches, fluid solutions were first obtained using Poisson's equation. The field from Poisson's equation was then compared to that from the quasineutral models. The field from the two fluid models presented here agreed well with Poisson's equation (up to the sheath edge) in all cases, but the field based on the Boltzmann relationship did not. Indeed, even the sign of the field from the Boltzmann relationship was wrong in some cases.

ACKNOWLEDGMENTS

The authors thank Dr. M. Lampe, Dr. W. Manheimer, and Professor R. Franklin for their insights and comments on various aspects of the problem. We are also grateful to Dr. D. Leonhardt, Dr. S. Walton, and Dr. R. Meger for sharing experimental results on plasmas produced by energetic elec-

tron beams. This work was supported by the Office of Naval Research.

APPENDIX A: EFFECTS OF A PERPENDICULAR MAGNETIC FIELD

Consider a weakly ionized plasma that varies with x only and is embedded in a uniform magnetic field $B\hat{y}$. Assume for simplicity that particles are created with zero net velocity on average (i.e., randomly in all directions) and are destroyed independent of velocity. Particle sources then add particles but not momentum to the ensemble, so the mean momentum $m_i u_i$ of the species as a whole decreases. The sinks, on the other hand, remove an average momentum equal to $m_i u_i$ per particle destroyed, and thus the mean momentum of the ensemble is unchanged. Hence, only the sources directly affect $m_i u_i$. Dropping the subscript i for convenience and assuming steady state, the momentum equations along x and z can therefore be written as

$$u_x \frac{du_x}{dx} = \frac{qeE}{m} - \frac{1}{mn} \frac{d(nT)}{dx} - \Omega u_z - (\nu + S_c/n)u_x \quad (\text{A1})$$

and

$$u_x \frac{du_z}{dx} = \Omega u_x - (\nu + S_c/n)u_z, \quad (\text{A2})$$

respectively. Here u_x is the flow velocity in the x direction, u_z is the flow velocity in the z direction, ν is the momentum-transfer collision frequency, $\Omega = qeB/mc$ is the cyclotron frequency, and S_c is the volumetric creation rate. We assume there is no flow along y .

In quasineutral regions u_x is less than the sound speed c_s , so the left-hand side of Eq. (A2) can be dropped provided $d/dx \ll \nu/c_s$. This condition is usually well met for electrons [31] (and even for ions at gas pressures above 100 mtorr). Equation (A2) then reduces to $u_z \rightarrow [\Omega/(\nu+S_c/n)]u_x$, while Eq. (A1) reduces to

$$u_x \frac{du_x}{dx} \rightarrow \frac{qeE}{m} - \frac{1}{mn} \frac{d(nT)}{dx} - Ru_x. \quad (\text{A3})$$

Here the effective momentum-loss rate along x is defined as

$$R \equiv \nu + \frac{S_c}{n} + \frac{\Omega^2}{\nu + S_c/n}. \quad (\text{A4})$$

The magnetic field thus increases R appreciably if the cyclotron frequency is large,

$$\Omega \gg (\nu + S_c/n). \quad (\text{A5})$$

APPENDIX B: CLOSED-FORM EXAMPLE

To illustrate the limitations of the Langmuir model, consider an ambipolar discharge ($I_c=0$) consisting of electrons (e) and one species of singly ionized, positive ions (p). Neglecting recombination, the net production rate for both species is given by $S_i = \alpha_e n_e$, where the electron avalanche rate α_e is taken as constant. If the discharge varies with x only but resides in a uniform magnetic field along \hat{y} , the electrons lose momentum along x at a rate given by $R_e = \nu_e + \alpha_e + \Omega_e^2/(\nu_e + \alpha_e)$, according to Appendix A. Here ν_e is the electron collision frequency and Ω_e is the electron cyclotron frequency. The magnetic field increases the ion momentum-loss rate as well, but the increase is much less because the ion cyclotron frequency is small, $\Omega_p \ll \Omega_e$. The magnetic field therefore reduces the effective electron mobility $\mu_e \equiv e/m_e R_e$ far more than the ion mobility $\mu_p \equiv e/m_p R_p$.

The densities and velocities of the electrons and ions are equal in the quasineutral interior, $n_e = n_p \equiv n$ and $u_e = u_p \equiv u$. Consequently, Eqs. (3) and (13) can be combined in steady state into a single, first-order differential equation

$$\frac{du}{dx} = \frac{\alpha_e c_s^2 + R_t u^2}{c_s^2 - u^2}. \quad (\text{B1})$$

Here $c_s \equiv \sqrt{(T_e + T_p)/(m_e + m_p)}$ is the sound speed and $R_t \equiv (m_e R_e + m_p R_p)/(m_e + m_p)$ is the total momentum-loss rate.

Because its numerator is positive definite, Eq. (B1) is singular when the Bohm condition is met, $u = \pm c_s$. Using that condition as a boundary condition at $x = \pm x_s$, we can immediately integrate Eq. (B1) to produce the transcendental solution

$$x(u) = \frac{c_s}{R_t} \left[\left(\frac{R_t + \alpha_e}{\sqrt{\alpha_e R_t}} \right) \tan^{-1} \left(\frac{u}{c_s} \sqrt{\frac{R_t}{\alpha_e}} \right) - \frac{u}{c_s} \right]. \quad (\text{B2})$$

The two boundary conditions make the problem overdetermined, however, and therefore α_e is not a free parameter but

an eigenvalue determined by setting $x(\pm c_s) = \pm x_s$. Using the continuity equation, one can show that the plasma density is given by

$$n(u) = n_o \left(\frac{\alpha_e c_s^2}{\alpha_e c_s^2 + R_t u^2} \right)^{(R_t + \alpha_e)/2R_t}, \quad (\text{B3})$$

where n_o is the plasma density at $x=0$.

Solutions (B2) and (B3) apply to the Langmuir model as well, but only in the limit that $m_e \rightarrow 0$ and $R_t \rightarrow R_p$. These restrictions arise because the Langmuir model is based on the Boltzmann approximation and thus cannot account for the momentum lost by the electrons. As a result, the Langmuir model overestimates both the ionization rate α_e and the power needed to maintain a magnetized plasma of density n_o . The errors are large if $B/P > 3$ G/mtorr, and even the sign of the electric field is wrong if B/P is much larger yet. In the latter case, the Bohm condition is no longer valid as a boundary condition, as discussed in Sec. VC.

APPENDIX C: NUMERICAL STABILITY

Maxwell's equations conserve the sum of the conduction and displacement currents, and therefore in media that vary along a single direction \hat{s} only,

$$\left[J(s,t) + \frac{1}{4\pi} \frac{\partial E}{\partial t} \right] A(s) = I_t(t). \quad (\text{C1})$$

Here the total current $I_t(t)$ depends on time t but not location s . Setting $J = \sigma E$ reduces Eq. (C1) to

$$\frac{\partial E}{\partial t} + 4\pi\sigma E = \frac{4\pi I_t(t)}{A(s)}. \quad (\text{C2})$$

This equation shows that the field relaxes at a rate $4\pi\sigma$, which indicates that explicit field solvers are stable only if the time step satisfies $\Delta t < (4\pi\sigma)^{-1}$. More generally $J = e \sum_i (q_i n_i u_i)$ in plasmas, where $\partial(n_i m_i u_i)/\partial t = q_i e n_i E + \dots$. Taking the time derivative of Eq. (C1) then gives

$$\frac{\partial^2 E}{\partial t^2} + \omega_p^2 E + \dots = \frac{4\pi}{A(s)} \frac{dI_t}{dt}, \quad (\text{C3})$$

where $\omega_p^2 = 4\pi e^2 \sum_i (q_i^2 n_i / m_i)$ is the plasma frequency squared. Hence, when time derivatives are retained in the velocity equations, explicit field solvers are stable only if the time step additionally satisfies $\Delta t < \omega_p^{-1}$. These restrictions apply to Poisson's equation as well, because it is equivalent to Eq. (C1) when the field is set to $E = -\partial\phi/\partial s$. Typically $4\pi\sigma \sim 10^3 n_e/P$ in unmagnetized plasmas, while $\omega_p \approx 6 \times 10^4 \sqrt{n_e}$. Here n_e is the electron density in cm^{-3} and P is the gas pressure (at room temperature) in mtorr.

Plasmas diffuse to the walls, however, in a time $\tau_d \approx x_w^2/D_a$, where x_w is the distance to the walls and $D_a \sim 10^6/P$ is the ambipolar diffusion coefficient in cm^2/s . The number of time steps needed to reach equilibrium is there-

fore often excessive: $N_s > (4\pi\sigma + \omega_p)\tau_d > 10^{-3}n_e x_w^2 \sim 10^{11}$ if, for example, $n_e = 10^{12} \text{ cm}^{-3}$ and $x_w = 10 \text{ cm}$.

To reduce the number of times steps, several changes were made in the simulations reported. The first was to solve Poisson's equation using a semi-implicit scheme like that proposed by Ventzek *et al.* [38] The second was to drop electron inertia from the left-hand side of Eq. (3b), which is justified to order $m_e u_e^2 / T_e \ll 1$. Ions alone then contribute to the plasma frequency ω_p appearing in Eq. (C3). To further accelerate the calculations, the ion densities were kept under

10^{11} cm^{-3} and the walls were moved in to $x_w = \pm 3 \text{ cm}$.

The quasineutral models drop the displacement current, so the conduction current $I_c = JA$ is constant instead. Only the source rates, collision frequencies, and Courant condition then limit Δt . Moreover, the grid spacing Δx can be much larger than the Debye length, while the Courant condition falls to $\Delta t < \Delta x / c_s$. Here the sound speed c_s is much less than the electron speed $\sqrt{T_e / 2\pi m_e}$ at the walls. The net result is that quasineutrality greatly reduces the stability restrictions on the time step Δt .

-
- [1] I. Langmuir, Phys. Rev. **33**, 954 (1929).
 [2] L. Tonks and I. Langmuir, Phys. Rev. **34**, 876 (1929).
 [3] D. W. Hewett, Comput. Phys. Commun. **84**, 243 (1994).
 [4] M. Lampe, G. Joyce, W. M. Manheimer, and S. P. Slinker, IEEE Trans. Plasma Sci. **26**, 1592 (1998).
 [5] F. F. Chen, *Introduction to Plasma Physics* (Plenum, New York, 1974), p. 66.
 [6] R. N. Franklin and J. Snell, J. Phys. D **32**, 1031 (1999).
 [7] E. R. Harrison and W. B. Thompson, Proc. Phys. Soc. London **74**, 145 (1959).
 [8] R. N. Franklin, *Plasma Phenomena in Gas Discharges* (Clarendon, Oxford, 1976) p. 56.
 [9] K.-U. Riemann, IEEE Trans. Plasma Sci. **23**, 709 (1995).
 [10] K.-U. Riemann, J. Phys. D **36**, 2825 (2003).
 [11] R. Fernsler, Bull. Am. Phys. Soc. **49**, 49 (2004).
 [12] R. Fernsler, Bull. Am. Phys. Soc. **48**, 60 (2003).
 [13] V. Midha and D. J. Economou, Plasma Sources Sci. Technol. **9**, 256 (2000).
 [14] M. Matsuoka and K. Ono, J. Vac. Sci. Technol. A **6**, 25 (1988).
 [15] W. M. Manheimer and R. F. Fernsler, IEEE Trans. Plasma Sci. **29**, 75 (2001).
 [16] G. L. Rogoff, J. Phys. D **18**, 1553 (1985).
 [17] L. D. Tsendin, Sov. Phys. Tech. Phys. **34**, 11 (1989).
 [18] R. N. Franklin and J. Snell, J. Plasma Phys. **64**, 131 (2000).
 [19] R. L. F. Boyd and J. B. Thompson, Proc. R. Soc. London, Ser. A **252**, 102 (1959).
 [20] A. J. Lichtenberg, M. A. Lieberman, I. G. Kouznetsov, and T. H. Chung, Plasma Sources Sci. Technol. **9**, 45 (2000).
 [21] N. St. J. Braithwaite and J. E. Allen, J. Phys. D **21**, 1733 (1988).
 [22] M. Lampe, G. Joyce, G. Ganguli, and V. Gavrishchaka, Phys. Plasmas **7**, 3851 (2000).
 [23] Alternatively, Eqs. (10a) and (11c) indicate that $E \rightarrow (dQ_c/ds)/(dk_s^2/ds)$ when $k_s^2 \rightarrow 0$. The field is then finite, since $dk_s^2/ds \neq 0$ at that location.
 [24] D. Bohm, in *The Characteristics of Electrical Discharges in Magnetic Fields*, edited by A. Guthrie and R. K. Wakerling (McGraw-Hill, New York, 1949), Chap. 3, p. 77.
 [25] J. E. Allen, Plasma Sources Sci. Technol. **13**, 48 (2004).
 [26] The requirement is less stringent in the plasma middle. There the flow velocities $u_i \rightarrow 0$, so the Boltzmann relationship applies to *all* species. Quasineutrality is then justified as long as ϕ varies slowly relative to the *total* Debye length λ_D instead.
 [27] M. J. Kushner, W. Z. Collison, and D. N. Ruzic, J. Vac. Sci. Technol. A **14**, 2094 (1996).
 [28] R. F. Fernsler, W. M. Manheimer, R. A. Meger, J. Mathew, D. P. Murphy, R. E. Pechacek, and J. A. Gregor, Phys. Plasmas **5**, 2137 (1998).
 [29] R. A. Meger, D. D. Blackwell, R. F. Fernsler, M. Lampe, D. Leonhardt, W. M. Manheimer, D. P. Murphy, and S. G. Walton, Phys. Plasmas **8**, 2558 (2001).
 [30] D. Leonhardt, S. G. Walton, D. D. Blackwell, W. E. Amatucci, D. P. Murphy, R. F. Fernsler, and R. A. Meger, J. Vac. Sci. Technol. A **19**, 1367 (2001).
 [31] W. M. Manheimer, R. F. Fernsler, M. Lampe, and R. A. Meger, Plasma Sources Sci. Technol. **9**, 370 (2000).
 [32] J. Dutton, J. Phys. Chem. Ref. Data **4**, 577 (1975).
 [33] H. W. Ellis, R. Y. Pai, E. W. McDaniel, E. A. Mason, and L. A. Viehland, At. Data Nucl. Data Tables **17**, 177 (1976).
 [34] L. G. Christophorou and J. K. Olthoff, J. Phys. Chem. Ref. Data **29**, 267 (2000).
 [35] G. D. Severn, X. Wang, E. Ko, and N. Hershkowitz, Phys. Rev. Lett. **90**, 145001 (2003).
 [36] R. N. Franklin, J. Phys. D **33**, 3186 (2000).
 [37] M. Lampe, W. M. Manheimer, R. F. Fernsler, S. P. Slinker, and G. Joyce, Plasma Sources Sci. Technol. **13**, 15 (2004).
 [38] P. L. G. Ventzek, R. J. Hoekstra, and M. J. Kushner, J. Vac. Sci. Technol. B **12**, 461 (1993).